

LIQUID SIDE MASS TRANSFER COEFFICIENT AND INTERFACIAL AREA AT VERTICAL LIQUID FLOW ON EXPANDED METAL SHEET PACKING

Zdeněk BROŽ and Mirko ENDRŠT

*Institute of Chemical Process Fundamentals,
Czechoslovak Academy of Sciences, 165 02 Prague - Suchbát*

Received October 8th, 1979

Prediction of the liquid side mass transfer coefficient k_1 at vertical liquid flow on the expanded metal packing is based on the penetration model according to Higbie. The experimental value of mass transfer coefficients k_1 at absorption of sparingly soluble gases with differing diffusivities in water (propane, carbon dioxide and helium) are in a good agreement with the predicted values in a wide range of linear wetting densities. Interfacial area is determined by the chemical method and is correlated by an empirical relation.

In design of separation units, it is necessary to know the interfacial area between the liquid and gas (vapour) and the liquid and gas side mass transfer coefficients. These quantities are determined for individual types of separation units empirically and their values depend predominantly on the way the interfacial area is formed. Here are considered separation units in which the interfacial area is formed by downward liquid flow on the geometric surface of internals. The relation is looked for between the hydrodynamics of liquid flow and liquid side mass transfer coefficient k_1 . As internals were frequently used stacked or dumped packings. Thus there exists a considerable volume of experimental material on the liquid side mass transfer coefficients k_1 and on the specific interfacial area a . Both quantities k_1 and a are usually presented graphically for the given geometric form, size of packing and physical properties of the liquid in dependence on the wetting density or are correlated by empirical relations. Their generalisation or even theoretical prediction is prevented by the complex nature of hydrodynamic liquid flow conditions determining both quantities. Hydrodynamic studies of liquid flow on random packings have given a number of useful informations on the magnitude of the total, dynamic and static holdups, on characteristics of flow in the core of the packing and in the vicinity of walls of the column, on residence time distribution of liquid in the packing *etc.*, but they have also demonstrated that the studied quantities are dependent on more parameters such as the ratio of packing size and diameter of the column, shape of the packing and its arrangement, contact angle and others. These studies contributed first of all to the understanding why the attempts for a more general and theoretically founded correlation have not been very successful. The complexity and variability of hydro-

dynamics of liquid flow on the surface of the packing is obviously caused by three-dimensional arrangement of random packings which allows the liquid flow "too many degrees of freedom." Considerable freedom in the direction and also in the flow characteristics (in a form of a film or streams) is manifested as the tendency to a nonuniform flow on the packing.

The experimenter has very few possibilities to observe the flow phenomena in the packing or to affect it and to study the consequences resulting from changes of hydrodynamics on the mass transfer coefficient k_1 . This evaluation of random packings holds obviously quite generally, but it much depends on actual conditions of geometry of the packing and equipment, physical properties and liquid or gas flow rates.

The packing internals in which are to a considerable degree suppressed the unwanted properties of random packings is the one formed by vertical parallel sheets of expanded metal. In case of a suitable arrangement there is no overflow of liquid between the sheets and on the walls of the unit, liquid flowing on the sheet is in a sufficiently wide range of linear wetting densities well distributed, flow on the packing can be observed visually and so considered its hydrodynamics. In the above given sense the hydrodynamics of liquid flow on the packing made of expanded metal can be considered simpler than with the random packing. The expanded metal packing is interesting also from the practical point of view of its application in separation units. High values of the liquid side volume mass transfer coefficient $k_1 a$ were determined at laboratory¹ and pilot plant unit^{2,3} conditions.

In this paper the liquid side mass transfer coefficient and interfacial area in relation to liquid flow hydrodynamics on the expanded metal packing of various geometries is studied. Experimental determination of interfacial area is used for expression of the liquid side mass transfer coefficient k_1 from the volumetric coefficient $k_1 a$. These experimental values of k_1 are then being compared with the values predicted in the theoretical part on basis of concepts on hydrodynamics of liquid flow on the vertical expanded metal packing.

THEORETICAL

Liquid side mass transfer coefficient k_1 depends on the mechanism of transport of the dissolved gas from the interface into the bulk of liquid. The basic models on mechanism of mass transfer lead to the film⁴, penetration^{5,6} and film-penetration models⁷ with various exponents on diffusivity in the range from 0.5 to 1. Selection of the suitable model could be made on basis of knowledge of hydrodynamics of liquid film flow on the expanded metal. The verified detailed description of hydrodynamics and thus of the transport mechanism from the interface is not available. As valuable proved visual observation of the liquid flow character on the packing and their comparison with the consideration on which the individual mass transfer models are based. The visual observation can be summarized as follows.

At high linear wetting densities Γ the whole geometric surface of the expanded metal, the mesh inclusive, is filled with uniformly flowing liquid film. Interfacial area is thus equal or close to the double of geometric surface area $A_g = 2Hl$. In each mesh of the expanded metal (Fig. 1) is visible an intensively stirred region, formed obviously by the downward flow of liquid streams on neighbouring ribs into the common point. We assume that at each process of downward flow a stirring of the liquid takes place from the interfacial area with the bulk of the film. From the geometry of the expanded metal (Fig. 1) results that the distance between individual stirrings of the interface with the bulk of the film should equal to one half of the vertical pitch diagonal. If we further assume that this process is repeated at time intervals Θ , which are so short that the film can be considered the semiinfinite space from the point of view of diffusion, this assumption leads to the penetration model according to Higbie⁴. The liquid side mass transfer coefficient k_1 obtained by solution of the unsteady state equation of diffusion into the semiinfinite space is given by equation

$$k_1 = (4D/\pi\Theta)^{1/2}. \quad (1)$$

The exposure time Θ is the parameter of the model and it is possible to assume that it is equal to the ratio of the length h after which the liquid mixing takes place and of the mean velocity of the liquid film v

$$\Theta = h/v. \quad (2)$$

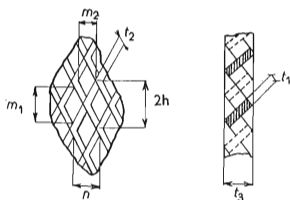


FIG. 1
Detail of Expanded Metal

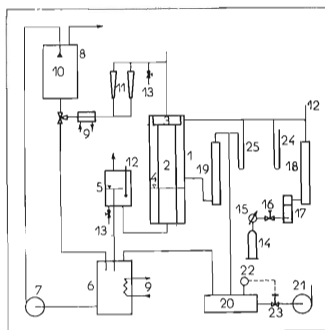


FIG. 2
Experimental Arrangement for Measurement of Interfacial Area

The average velocity of the liquid film is calculated from the linear wetting density Γ and the total liquid holdup per unit of geometric area of the expanded metal z

$$v = \Gamma/z. \quad (3)$$

After substitution of Eqs (2) and (3) into Eq. (1) the relation is obtained

$$k_1 = (4D\Gamma/(\pi h z))^{1/2} \quad (4)$$

including the characteristic dimension of the expanded metal, gas diffusivities in liquid, linear wetting density and total liquid holdup. For the total liquid holdup Tesař ad Kolář⁸ have proposed the relation

$$z = (\varphi \mu_1 \rho_1 \Gamma / g)^{1/3} \quad (5)$$

based on the Nusselt's⁹ relation for the thickness of film at vertical liquid flow on the flat plate. Relation (5) holds for the case when the holdup is not affected by gas flow. The effect of geometry of the expanded metal is included into the empirical coefficient φ . By substitution of Eq. (5) into (4) the relation is obtained

$$k_1 = (4D/(\pi h))^{1/2} (g/(\varphi \mu_1 \rho_1))^{1/6} \Gamma^{1/3} \quad (6)$$

TABLE I

Expanded Metal Sheets. All length dimensions are in mm.

Specification		10 × 5 stainless steel	16 × 6 stainless steel	28 × 8 steel
Vertical pitch diagonal	$2h$	10	16.5	28.2
Horizontal pitch diagonal	n	4.5	5.5	8
Vertical mesh diagonal	m_1	7.5	11.5	22
Horizontal mesh diagonal	m_2	2	3.3	5.7
Thickness of metal	t_1	0.35	0.5	0.7
Thickness of ribs	t_2	1.6	1.2	1.5
Thickness of expanded metal	t_3	1.6	2	2.1
Plate width	l	65	63	63
Coeff. in Eq. (5)	φ	44.6	16.9	8.61
Coeff. in Eq. (9)	α_∞	1.05	1.075	0.925
	α_0	0.3	0.35	0.3
	β	12	8.4	5

Comparison of relation (6) with the experimental k_1 values is made in the experimental part of this study. The effect of viscosity, specific density and surface tension has not been studied systematically.

EXPERIMENTAL

For measurements, three expanded metals were used with the geometric dimensions given in Fig. 1 and Table I. The interfacial areas A have been measured by the chemical method and k_1A by physical absorption of sparingly soluble gases with various diffusivities in water (propane, carbon dioxide and helium). Both measurements were performed in the same rectangular column $80 \times 16 \times 750$ mm on the same plates made of expanded metal. The liquid side mass transfer coefficients k_1 were calculated under the assumption that the interfacial area A determined by the chemical method for the given linear wetting density is identical with the value at physical absorption. Specifications of the arrangement of the apparatus for measurement of interfacial area and physical absorption rates are also given.

Interfacial area. Interfacial area has been determined under the conditions of fast pseudo first order reaction at the absorption of pure humidified carbon dioxide at lowered pressure into solutions of sodium hydroxide in the apparatus given in Fig. 2. Into absorption column 1 has been inserted a strip of expanded metal 2 equipped with slotted distributor 3 and was stretched by tension toward the lower flange so that it has not been in touch with the walls. The length of the film H of liquid flowing on the expanded metal could be fixed according to the height of liquid 4 in the column by use of a movable external overflow 5. From the overflow the liquid was flowing into the 100 l storage tank 6. The bellow pump 7 was used for pumping the solution into the upper storage tank 8 and for its circulation. The solution was thermostated 9 and degassed by spraying through a jet 10 which lasted for about four hours at the pressure 5 kPa. The liquid flow rate was measured by calibrated rotameters 11. The inlet and outlet temperatures 12 and the composition of solution 13 were measured. Carbon dioxide from the pressure flask 14 after pressure control 15 passed through the needle valve 16 and after humidification in the thermostated washing flask with the sintered glass distributor 17 entered into the gas burette 18 having the volume 1750 ml. The excess of unabsorbed gas (about a half) was measured by the gas burette 19 (volume 500 ml) and left through the intermediate tank 20 into the vacuum pump 21. The pressure in the intermediate tank was controlled by mercury manostat with the memory 22 by use of the solenoid valve 23. Pressure in the apparatus was measured by the mercury manometer 24. Pressure in the outlet burette was controlled by the waterfilled U-manometer 25. Temperature of the gas in the outlet burette was approx. equal to the mean temperature of liquid in the column. The gas flow rates through the burettes were measured by the stop watch. Partial pressure of carbon dioxide was computed from the pressure in the apparatus and partial pressure of water vapour above the solution at the given temperature and was approx. equal to 10 kPa. Concentration of sodium hydroxide in the solution was approx. $c_B = 700 \text{ mol m}^{-3}$ and the conditions of the regime of fast pseudo-first order reaction were satisfied¹⁰. At these conditions for the rate of absorption the relation holds

$$RA' = A'c_{Aw}(k_2c_B D_A)^{1/2}, \quad (7)$$

where $A' = A + 0.0012 \text{ m}^2$ is the sum interfacial areas of the liquid film on the expanded metal and the liquid surface at the outlet. Solubility of carbon dioxide in the solution, rate constant of reaction and diffusivity were taken from literature¹⁰ together with usual corrections on the effect of ionic strength of solution. Analysis of the solution prepared from distilled water and

sodium hydroxide analytical grade reagents was performed by the titration method according to Warder for determination of hydroxides and sodium carbonates.

The results of measurements of interfacial area expressed in the dimensionless relative interfacial area

$$\alpha = A/A_g \quad (8)$$

are plotted in Fig. 3. For the expanded metal sheets denoted as 16×6 are given average values of repeated measurements for two film lengths $H = 0.37$ and 0.67 m. It can be seen from this figure that differing lengths of the film do not have any effect on the relative interfacial area α . For further evaluation, the experimental dependence was approximated by the empirical relation

$$\alpha = \alpha_\infty - (\alpha_\infty - \alpha_0) \exp(-\beta l) \quad (9)$$

The values of parameters α_∞ , α_0 and β are given in Table I. For expanded metal sheets 10×5 and 28×8 are given in Fig. 3 only dependences according to Eq. (9). The asymptotes $\alpha_\infty = 1.05$ and 1.075 for large values of l for expanded metal sheets 10×5 and 16×6 are in agreement with the increase of interfacial area due to the existence of waves on the fully covered geometric surface at the used wetting densities.

Physical absorption. Physical absorption of individual gases into the de-gassed water at approx. 25°C was performed at atmospheric pressure. The arrangements of the apparatus are obvious from Fig. 4 and they concern the measurements of flow rates and composition of the absorbed gas. Gas from the pressure flask 14 after pressure control 15 passed through the solenoid valve 24

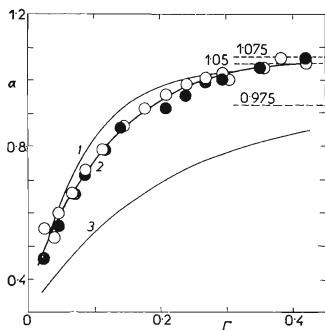


FIG. 3

Relative Interfacial Area in Dependence on Linear Wetting Density

1 Expanded metal 10×5 ; 2 expanded metal 16×6 , $\circ H = 0.37$ m, $\bullet H = 0.67$ m; 3 expanded metal 28×8 .

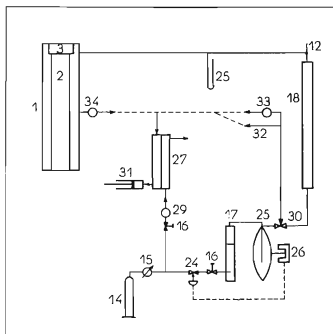


FIG. 4

Arrangements of Experimental Device for Measurement of Physical Absorption

and needle valve 16 into the thermostated washing bottle with sintered glass distributor 17 and into the rubber bulb 25. Photoelectric sensor 36 controlled the gas inlet into the bulb by use of the solenoid valve 24. Volume of the gas burette 18 was chosen according to solubility and

TABLE II
Diffusivity and Solubility of Propane, Carbon Dioxide and Helium in Water at 25°C

Properties of gases	Propane	Carbon dioxide	Helium
Diffusivity $D \cdot 10^9, \text{m}^2 \text{s}^{-1}$	1.16 (ref. ^{11,12})	1.92 (ref. ¹³)	6.28 (ref. ¹³)
Mole fraction of gas $X \cdot 10^4$ in water at pressure $P = 1.01325 \cdot 10^5 \text{ Pa}$	0.270 (ref. ¹⁴)	6.111 (ref. ¹⁴)	0.07046 (ref. ^{14,15})
Henry law constant (calc) $H \cdot 10^{-9}, \text{Pa}$	3.749	0.1658	14.38

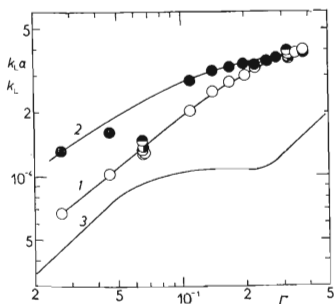


FIG. 5

Dependence of $k_1\alpha$ and k_1 on Linear Wetting Density at Absorption of Carbon Dioxide in Water on Expanded Metal Sheets 16×6 and on Smooth Plate

1 $k_1\alpha$ expanded metal 16×6 , film length $H = 0.1 \text{ m}$ ○, $H = 0.24 \text{ m}$ ●, $H = 0.52 \text{ m}$ ⊙, $H = 0.67 \text{ m}$ ○; 2 k_1 expanded metal 16×6 ; ● $H = 0.67 \text{ m}$; 3 $k_1\alpha$ smooth plate.

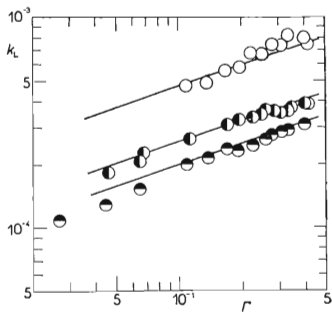


FIG. 6

Dependence of k_1 on Linear Wetting Density on Expanded Metal Sheets 10×5 , Film Length $H = 0.37 \text{ m}$

● Propane, ● carbon dioxide, ○ helium.

diffusivity of gas in water (Table II). For the absorption rate on infinitesimal interfacial area $\alpha \, dA_g$ holds relation

$$(\Gamma/lq_1) \, dc_b = k_1(c_w - c_b) \, \alpha \, dA_g. \quad (10)$$

By integration at the assumption of zero concentration of the absorbed gas in liquid at the inlet $c_{b1} = 0$, plug flow of liquid, constant values c_w , α and k_1 along the height, relation results

$$k_1\alpha = (\Gamma/(2q_1H)) \ln 1/(1 - c_{b2}/c_w). \quad (11)$$

The accuracy of determination of $k_1\alpha$ depends first of all on the accuracy with which the ratio c_{b2}/c_w is determined. The outlet concentration c_{b2} was calculated from the volume flow rate of the absorbed gas V by gas burettes. The equation for c_{b2} has the form

$$c_{b2} = (1 - y_{1i} - y_{1v}) PVq_1/(RTl). \quad (12)$$

Mole fractions of inert gas (air) and water vapour in the gas flowing in the burettes were measured by the Zeiss interferometer 27. As the standard gas was used the continuous supply of dried gas from the pressure flask on silicagel 29. Gas from the three way cock 30 was sucked into the measuring chamber of interferometer by the injection syringe 31 or directly 32 or over drying silicagel 33.

Concentration of the absorbed gas on interface c_w was calculated from the Henry's law constant

$$c_w = (1 - y_{2i} - y_{2v}) Pq_1/(\mathcal{R}M_1) \quad (13)$$

for the average liquid temperature and composition of gas in the column. In the gas sample withdrawn from the column 1 and dried by silicagel 34 was determined the mole fraction of inert gas. The content of water vapour was calculated from the water vapour pressure at the given temperature. The content of inert gas in column 1 depended on the degree of degassing of water. Degassing of water was performed also at 5 kPa for about four hours.

RESULTS

The averaged values of repeated measurements of $k_1\alpha$ of absorption of carbon dioxide on the expanded metal sheets 16×6 calculated from Eqs (11) up to (13) are given in Fig. 5 and are compared with the results obtained earlier on the smooth plate². Solid lines are curves drawn through experimental points. The effect of the film length on the value $k_1\alpha$ was studied at two linear wetting densities $\Gamma = 0.065$ and $0.32 \, \text{kg m}^{-1} \text{s}^{-1}$. A significant effect of systematic errors on $k_1\alpha$ was not found for film lengths $H = 0.1; 0.24; 0.37; 0.52$ and $0.67 \, \text{m}$. In Fig. 5 is also given the liquid side mass transfer coefficient k_1 calculated from $k_1\alpha$ and the relative interfacial area α by use of empirical relation (9). At small values of linear wetting density, the coefficient k_1 is larger than $k_1\alpha$ because α is smaller than one as is obvious from Fig. 3.

Similar dependences were obtained for other gases used and all expanded metal sheets. In Figs 6 to 8 are given values of the coefficient k_1 for individual gases in comparison with solid lines calculated from Eq. (6). The measurements on the expanded metal sheet 10×5 (Fig. 6) were performed only for the length of the film $H = 0.37 \, \text{m}$.

The agreement of the measured and calculated values is very good first of all at larger values of linear wetting densities. For smaller values the ratio c_{b2}/c_w is close to one and results in a larger spread of the values k_1 . Thus in the case of absorption of helium, which has a large diffusivity in water, the measurements at small wetting densities are not given. Measurements of the expanded metal sheets 16×6 (Fig. 7) also demonstrate a good agreement with the estimates for propane, carbon dioxide and helium. In the case of expanded metal sheets 28×8 (Fig. 8) the experimental values of the coefficient k_1 are higher by about 20% than the estimated values. From quantities appearing in Eq. (4) and having the effect on k_1 the holdup was calculated from empirical relation (5). The length h , on which the liquid was completely mixed from the interface with the bulk of liquid, was taken as one half of vertical pitch diagonal of the expanded metal sheets. The made assumption on the length h can be also considered by arrangements of Eq. (4) and by evaluation of the empirical parameter h_{emp} from experimental data by use of Eq. (14).

$$h_{emp} = 4D\Gamma/(\pi z k_L^2) \quad (14)$$

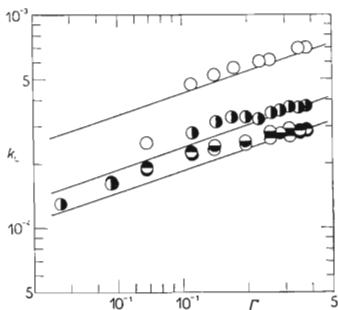


FIG. 7

Dependence of k_1 on Linear Wetting Density on the Expanded metal 16×6

$H = 0.37 \text{ m} \quad 0.67 \text{ m}$

Propane	●	●
Carbon dioxide	◐	◑
Helium	○	

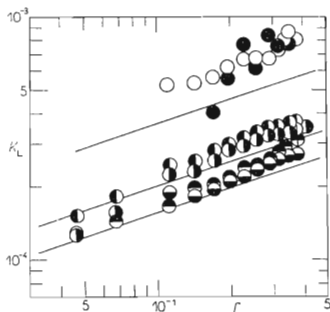


FIG. 8

Dependence of k_1 on Linear Wetting Density on Expanded Metal 28×8

$H = 0.37 \text{ m} \quad 0.67 \text{ m}$

Propane	●	●
Carbon dioxide	◐	◑
Helium	○	●

In Fig. 9 are plotted for individual expanded metal sheets the averaged values h_{emp} for all absorbed gases. This is possible because, as from Figs 6–8 results, the experimental data of individual gases comply with the penetration model according to Higbie Eq. (1) with the dependence of the coefficient k_1 on diffusivity with the exponent equal to one half. From Fig. 9 and Table I results that, at high linear wetting densities Γ is the calculated empirical parameter h_{emp} equal or slightly smaller than one half of the vertical pitch diagonal. In the case of expanded metal sheet 28×8 is closer to one half of the mesh diagonal. At high values of Γ were obviously best satisfied the assumptions made in the theoretical part of this study. At small values of Γ the value h_{emp} increases. On the expanded metal sheets the hydrodynamics is affected, the relative interfacial area α considerably decreases, distribution of flow becomes eventually irregular and deviations from the assumption of plug flow appear, the value of the substituted holdup becomes uncertain, and deviations from the assumption on equality of interfacial area at chemical and physical absorption can be encountered. Without further experimental material a detailed analysis of the obtained dependences has no sense. The data on absorption of carbon dioxide on smooth plate are for illustration evaluated in a similar manner in Fig. 9. The calculated values of h_{emp} are for the smooth plate considerably larger. Special shape of curves obviously results from the existence of laminar, transition, and turbulent regimes. In all figures the linear wetting density Γ was purposely used as the independent variable even though it is possible to use the Reynolds number. The effect of physical properties of liquids is considered in the next study of this series.

The valuation of experimental data on absorption of sparingly soluble gases with

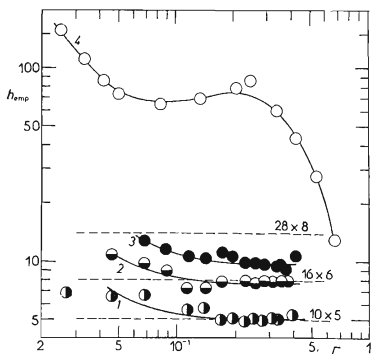


FIG. 9
Dependence of Empirical Parameter h_{emp}
on Linear Wetting Density
1 ● expanded metal 10×5 ; 2 ● expanded
metal 16×6 , 3 ● expanded metal 28×8 ,
4 ○ smooth plate¹.

differing diffusivities into water film on expanded metal sheets of various dimensions proved that the liquid side mass transfer coefficient can be predicted on basis of experimental data on hydrodynamics and penetration model according to Higbie⁵. Another of the known penetration models such as *e.g.* the Danckwert's surface renewal model⁶ leads to the relation

$$k_1 = (Ds)^{1/2}. \quad (15)$$

The empirical parameter — intensity of surface renewal s evaluated from Eq. (15) cannot be so easily hydrodynamically interpreted as the time of exposure θ according to the Higbie model.

LIST OF SYMBOLS

a	specific interfacial area (m^{-1})
A	interfacial area on the expanded metals sheets (m^2)
A'	interfacial area on the expanded metal sheets liquid surface at the outlet inclusive (m^2)
$A_g = 2HI$	geometric surface area of the expanded metal sheets (m^2)
c	concentration (mol m^{-3})
D	diffusivity of gas in liquid ($\text{m}^2 \text{s}^{-1}$)
g	gravitational acceleration (m s^{-2})
h	half of vertical pitch diagonal (m)
H	length of liquid film (m)
$\mathcal{H} = P/x$	Henry law constant (Pa)
k_1	liquid side mass transfer coefficient (ms^{-1})
l	width of expanded metal plate (m)
M	molecular mass (kg mol^{-1})
P	total pressure (Pa)
R	gas law constant ($8.314 \text{ J mol}^{-1} \text{ K}^{-1}$)
R	absorption rate per unit of interfacial area ($\text{mol m}^{-2} \text{ s}^{-1}$)
s	intensity of surface renewal (s^{-1})
T	absolute temperature (K)
v	mean velocity of liquid film defined by Eq. (3) (m s^{-1})
V	volumetric flow rate of gas through the burette ($\text{m}^3 \text{ s}^{-1}$)
x	mole fraction of component in liquid (—)
y	mole fraction of component in gas (—)
z	total holdup (kg m^{-2})
α	relative interfacial area defined by Eq. (8) (—)
α_0	relative interfacial area at $\Gamma = 0$ (—)
α_∞	relative interfacial area, asymptote at $\Gamma \rightarrow \infty$ (—)
β	empirical coefficient in Eq. (9) ($\text{kg}^{-1} \text{ m s}$)
Γ	linear wetting density ($\text{kg m}^{-1} \text{ s}^{-1}$)
φ	empirical coefficient in Eq. (5) (—)
μ	dynamic viscosity ($\text{kg m}^{-1} \text{ s}^{-1}$)
ρ	specific density (kg m^{-3})

Subscripts

A	carbon dioxide
B	hydroxide ions
b	bulk
emp	empirical
i	inert (air)
l	liquid
v	water vapour
w	interface
1	inlet
2	outlet

REFERENCES

1. Kolář V., Endršt M.: *This Journal* 38, 359 (1973).
2. Endršt M., Červenka J., Kolář V.: *Chem. Prům.* 25, 50, 138 (1975).
3. Kolář V., Lacina J.: *This Journal* 45, 1343 (1980).
4. Whitman W. G.: *Chem. Met. Eng.* 29, 147 (1923).
5. Higbie R.: *Trans. Amer. Inst. Chem. Eng.* 31, 65 (1935).
6. Danckwerts P. V.: *Ind. Eng. Chem.* 43, 1460 (1951).
7. Toor H. L., Marchello J. M.: *AIChE J.* 4, 97 (1958).
8. Tesaf A., Kolář V.: *This Journal* 42, 3301 (1977).
9. Nusselt W.: *Z. Ver. Dtsch. Ing.* 60, 541 (1916).
10. Danckwerts P. V.: *Gas-Liquid Reactions*. McGraw-Hill, New York 1970.
11. Hayduk W., Laudie H.: *AIChE J.* 20, 611 (1974).
12. Witherspoon P. A., Bonoli L.: *Ind. Eng. Chem. Fundam.* 8, 589 (1969).
13. Himmelblau D. M.: Ferrell R. T.: *AIChE J.* 13, 702 (1967).
14. Wilhelm E., Battino R., Wilcock J.: *Chem. Rev.* 77, 219 (1977).
15. Benson B. B., Krause D. J.: *J. Chem. Phys.* 64, 689 (1976).

Translated by M. Rylek.